Published in final edited form as:
Virology. 2007 June 20; 363(1): 113–123.

Mapping and restriction of a dominant viral CD4+ T cell core epitope by both MHC class I and MHC class II

Dirk Homann[a,*], **Hanna Lewicki**[b], **David Brooks**[b], **Jens Eberlein**[a], **Valerie Mallet-Designé**[c], **Luc Teyton**[c], and **Michael B.A. Oldstone**[b,d,*]

a*Barbara Davis Center, University of Colorado at Denver and Health Sciences Center, 12801 East 17th Avenue, Aurora CO, USA*

b*Department of Molecular and Integrative Neurosciences, The Scripps Research Institute, 10550 N. Torrey Pines Road, La Jolla CA, USA*

c*Department of Immunology, The Scripps Research Institute, 10550 N. Torrey Pines Road, La Jolla CA, USA*

d*Department of Infectology, The Scripps Research Institute, 10550 N. Torrey Pines Road, La Jolla CA, USA*

Abstract

Virus-specific $CD4^+$ T cells contribute to effective virus control through a multiplicity of mechanisms including direct effector functions as well as "help" for B cell and $CD8^+$ T cell responses. Here, we have used the lymphocytic choriomeningitis virus (LCMV) system to assess the minimal constraints of a dominant antiviral $CD4^+$ T cell response. We report that the core epitope derived from the LCMV glycoprotein (GP) is 11 amino acids in length and provides optimal recognition by epitope-specific $CD4^+$ T cells. Surprisingly, this epitope is also recognized by LCMV-specific $CD8^+$ T cells and thus constitutes a unique viral determinant with dual MHC class I- and II-restriction.

Keywords

Virus; LCMV; T cell response; CD4; CD8; MHC class I; MHC class II

Introduction

Effective control of microbial infections, in particular viruses, relies on the concerted activity of pathogen-specific T and B cells. While the relative contribution of individual immune cell subsets depends on the precise determinants of host-pathogen interaction (nature of the pathogen, route of pathogen entry, pathogen dosage and host immune status), $CD8^+$ T cells and B cells constitute the main effector cell populations in most viral infections (Burton, 2002; Whitton and Oldstone, 2001; Zinkernagel, 2002). In contrast, antiviral $CD4^+$ T cell responses are for the most part significantly smaller than $CD8^+$ T cell responses and may wane over time (Seder and Ahmed, 2003; Sprent and Surh, 2002). Nevertheless, $CD4^+$ T cells play a critical and multifaceted role at all stages of the adaptive immune response by serving as effectors, helpers and/or regulators/supressors.

Direct antiviral effector functions elaborated *in vivo* by specific $CD4^+$ T cells include the production of cytokines and chemokines and possibly cytotoxic T cell activity (Appay, 2004; Jenkins et al., 2001; Seder and Paul, 1994). The traditional designation of $CD4^+$ T cells as

*Corresponding authors. M.B.A. Oldstone is to be contacted at Department of Molecular and Integrative Neurosciences, The Scripps Research Institute, 10550 N. Torrey Pines Road, La Jolla CA, USA..
E-mail addresses: dirk.homann@uchsc.edu (D. Homann), mbaobo@scripps.edu (M.B.A. Oldstone).

"helper T cells" is based on their importance for enhancement and modulation of specific antibody responses (McHeyzer-Williams et al., 2003), but work over the past few years has made increasingly clear that additional help is also provided to $CD8^+$ T cell responses (reviewed, Bevan, 2004). Here, the relevant molecular interactions remain to be elucidated in detail but it appears that, depending on the *in vivo* model system under study, induction of primary $CD8^+$ T cell responses, generation and maintenance of $CD8^+$ T cell memory as well as secondary $CD8^+$ T cell immunity are all improved by the activity of specific $CD4^+$ T cells (Bevan, 2004; Homann, 2002). The complex function of antiviral $CD4^+$ T cell immunity is further supported by studies on relevant human diseases such as HIV, EBV, CMV, HBV and HCV infections (Norris and Rosenberg, 2002). Altogether, it may be said that the relative importance of antigen-specific $CD4^+$ T cell responses increases with the extent of viral disease (viral load and associated inflammatory alterations) (Homann, 2002). Finally, in their incarnation as "regulatory T cells", $CD4^+$ T cells are actively engaged in curtailing immune responses which may have beneficial (limitation of immunopathology) or adversarial (incapacitation of $CD8^+$ T cell responses) effects (Belkaid and Rouse, 2005; Dittmer et al., 2004; Mittrucker and Kaufmann, 2004).

In the present study, we have employed the lymphocytic choriomeningitis virus (LCMV) system to further define the nature of antiviral $CD4^+$ T cell responses (Homann et al., 2001; Kamperschroer and Quinn, 1999; Lenz et al., 2004; Oxenius et al., 1995; Varga and Welsh, 1998a, 1998b, 2000; Whitmire et al., 1998). Originally identified by Oxenius et al. (1995) the immunodominant population of LCMV-specific $CD4^+$ T cells in C57Bl/6J mice targets an epitope derived from the viral glycoprotein ($GP_{61–80}$) and restricted by I-A^b. Here, we have used several $GP_{61–80}$-specific $CD4^+$ T cell lines and clones, a battery of truncated peptides from the $GP_{61–80}$ epitope and surface plasmon resonance to determine the minimal constraints and avidities of a dominant, virus-specific T cell receptor (TCR)–MHC interaction.

Results

Generation of LCMV-specific $CD4^+$ T cell lines and clones

To generate $CD4^+$ T cell lines and clones specific for the I-A^b-restricted LCMV $GP_{61–80}$ epitope, a C57Bl6/J mouse was infected with LCMV Armstrong clone 53b (1.5×10^5pfu i.p.) to induce LCMV-specific T cell responses and virus clearance. Thirteen days later, spleen cells were isolated, depleted of $CD8^+$ T cells and cultured in the presence of $GP_{61–80}$ peptide as detailed in Materials and methods. Forty $CD4^+$ T cell lines and/or clones were established and tested for TCR usage and IFNγ production, a hallmark of LCMV-specific $CD4^+$ T cells (Homann et al., 2001; Kamperschroer and Quinn, 1999; Varga and Welsh, 1998a; Whitmire et al., 1998). As about 1/3 of $GP_{61–80}$-specific effector (data not shown) and memory (Homann et al., 2001) $CD4^+$ T cells utilize Vβ8.1/8.2 TCRs, we selected 6 cell lines/clones for further analysis based on Vβ8.1/8.2 and Vα2 TCR expression as well as efficient IFNγ induction after resting and restimulation with $GP_{61–80}$ peptide (Figs. 1 and 2B).

Differential I-$A^b$$GP_{61–80}$ binding by $CD4^+$ T cell lines and clones

We subsequently evaluated the selected cell lines/clones for their ability to bind I-$A^b$$GP_{61–80}$ tetramers. Here, three distinct staining patterns emerged: (1) efficient tetramer binding (clones #3 and #31), (2) partial tetramer binding indicative of more than one TCR specificity present in the cell preparation (cell lines #21 and #32) and (3) absence of tetramer binding (clones/cell lines #8 and #35) (Fig. 2A). To evaluate if effective tetramer staining could be "rescued", we used a more sensitive staining technique, tetramers deployed on fluorescent liposomes (Mallet-Designé et al., 2003). Although this approach reliably improved the "signal-to-noise ratio" for clones #3 and #31, it demonstrated only slight staining above background levels for clones/cell lines #8, #21 and #35 (Fig. 2A). Furthermore, tetramer binding did not

demonstrate any appreciable correlation with the extent of TCR or CD4 co-receptor expression on the cell surface as determined by measuring the mean fluorescent intensity of Vβ8.1/8.2, Vα2 and CD4 staining (Fig. 2B and data not shown).

Identification of an 11 amino acid core epitope ($GP_{67–77}$)

In spite of their differential ability to bind MHC class II tetramers, the prompt induction of IFNγ production in the selected cell lines/clones (#3, #8, #21, #31, #32, #35) made this functional assay suitable to determine the minimal constraints of I-A^b-restricted $GP_{61–80}$ epitope presentation and TCR reactivity. Using a panel of truncated peptides and comparing the extent of IFNγ induction to that elicited by the native $GP_{61–80}$ peptide, we identified a core motif of 11 amino acids ($GP_{67–77}$) that on average induces 2/3 of the maximal IFNγ response in the 6 cell lines/clones (Fig. 3A). When tested on primary LCMV-specific $CD4^+$ T cells (8 days after LCMV infection), the $GP_{67–77}$-specific response was consistently of slightly greater magnitude as compared to $GP_{61–80}$- or $GP_{64–80}$-specific responses (Fig. 3B). These results indicate that flanking residues of the core epitope present in the $GP_{61–80}$ and $GP_{64–80}$ peptides may preclude recognition of the epitope by a subset of virus-specific $CD4^+$ T cells and identify $GP_{67–77}$ as the immunodominant LCMV-specific, I-A^b-restricted $CD4^+$ T cell core epitope.

Restriction of the core epitope $GP_{67–77}$ by both I-A^b and D^b

During our analyses of peptide-induced IFNγ production by primary murine effector $CD4^+$ T cells (Fig. 3A), we noted unusually high “background staining” in CD4-negative cells obtained from cultures stimulated with GP_{67} but not GP_{64} or NP_{309} peptides (Fig. 4A). We therefore evaluated the possibility that the $GP_{67–77}$ epitope may also be recognized in an MHC-I-restricted fashion by LCMV-specific $CD8^+$ T cells. In B6 mice, the majority of specific $CD8^+$ T cells recognize two co-dominant epitopes restricted by D^b ($GP_{33–41}$ and $NP_{396–404}$) as well as two subdominant epitopes restricted by D^b and K^b, respectively ($GP_{276–286}$ and $GP_{34–43}$) (Gairin et al., 1995;Hudrisier et al., 1997;Klavinskis et al., 1990;Oldstone et al., 1988;Schulz et al., 1989). More recently, several additional subdominant epitopes have been identified and include the epitopes $GP_{92–101}$ and $NP_{166–175}$ (D^b-restricted) as well as $GP_{118–125}$, and $NP_{205–212}$ (K^b-restricted) (van der Most et al., 2003;van der Most et al., 1998). Indeed, we found that the $GP_{67–77}$ epitope is recognized by both LCMV-specific $CD4^+$ and $CD8^+$ T cells (Fig. 4B) and that D^b is the restriction element for specific $CD8^+$ T cell responses (Fig. 4C) Thus, the $GP_{67–77}$ epitope constitutes a rather unique viral determinant as it is targeted, by virtue of its dual restriction, by both $CD4^+$ and $CD8^+$ T cell populations. Furthermore, since stimulation with the $GP_{64–80}$ peptide was not associated with IFNγ induction in $CD8^+$ T cells unless provided at excessively high concentrations (50 μg/ml, data not shown), the presence of the 3 additional carboxy-terminal ($GP_{64–66}$) and amino-terminal ($GP_{78–80}$) residues apparently interferes with effective D^b-restricted presentation.

Finally, the distribution of $GP_{67–77}$-specific T cells among $CD4^+$ and $CD8^+$ T cell subsets was found to be about similar with 45–50% of $GP_{67–77}$-reactive T cells expressing either CD4 or CD8 and a minority of T cells specific for this epitope (<10%) expressing both co-receptors (Fig. 4D).

TCR Vβ usage and functional avidities of primary I-A^b and D^b-restricted $GP_{67–77}$-specific T cells

To assess the distribution of TCR usage by $GP_{67–77}$-restricted $CD4^+$ and $CD8^+$ T cells, we utilized a panel of TCR Vβ-specific antibodies in conjunction with intracellular IFNγ staining. $GP_{67–77}$-specific $CD4^+$ T cells were preferentially recruited from just two TCR Vβ families (8.1/8.2 and 14) with several other TCR Vβ families contributing less than 5% each to the overall $GP_{67–77}$-restricted $CD4^+$ T cell response. In contrast, $GP_{67–77}$-specific $CD8^+$ T cells appeared more diversified as indicated by five TCR Vβ families (2, 8.1/8.2, 8.3, 9, 10)

contributing >5% to the overall specific response as well as larger error bars in the bar diagram reflective of differential private TCR Vβ usage among individual mice (Fig. 5A).

We and others have previously reported that the functional avidities of LCMV-specific $CD4^+$ T cells (measured by determining the reciprocal peptide concentration required for IFNγ induction in half of an epitope-specific T cell population) are considerably lower than those of LCMV-specific $CD8^+$ T cells (Homann et al., 2002; 2001; Whitmire et al., 2006). However, a careful interpretation of such data has to consider that induction of effector functions in this assay is dependent on both T cell-intrinsic properties ("functional avidities") as well as differential binding affinities of synthetic peptides to MHC class I or II molecules ("structural aviditities"). Our observation of virus-specific $CD4^+$ and $CD8^+$ T cells responses specific for the same peptide epitope now allows for a more direct comparison of functional avidities between these cell lineages and indicates comparable functional avidities of $GP_{67–77}$-specific $CD4^+$ and $CD8^+$ T cell populations (Fig. 5B).

Fitting of the core epitope $GP_{67–77}$ to I-A^b motifs

Based on the identity of naturally processed I-A^b peptides and the recently solved of I-A^b crystal structure (Dongre et al., 2001; Zhu et al., 2003), we proposed a common I-A^b-restricted peptide-binding motif. When applied to the LCMV-GP sequences, we found that no optimal alignment could be detected for the 11-mer $GP_{67–77}$ peptide or longer variants of the same peptide (Fig. 6A). Attempts to optimize the two most likely sequence alignments (K-Y-F-V and Y-V-Q-S for P1-P4-P6-P9, respectively) by substituting non-optimal residues with canonical residues at the same position failed to produce better agonistic peptides (Fig. 6B and LT/MBAO, unpublished). The absence of an optimum register for the GP peptide suggests that like in the case of I-A^d and I-Ag^7, peptides bound to I-A^b can adopt different alternate registers of binding (Corper et al., 2000; Scott et al., 1998). This capacity to use alternate registers has two practical consequences: (i) lower peptide affinity for the MHC and (ii) increase the repertoire of peptides from any given pathogen and therefore increase T cell repertoire against this pathogen. In the case of LCMV, the usage of this strategy to increase the efficiency of the anti-viral response appears very appropriate.

Binding affinity of LCMV-specific $CD4^+$ T cell receptors

Having determined the minimal requirements for $GP_{61–80}$ epitope binding and recognition, we proceeded to investigate in more detail the binding affinity of selected $CD4^+$ T cell clones. To this extent, PCR products from clones #3 and #31 were inserted into the pCR2.1-TOPO cloning vector and sequenced. Both I-A^b tetramer-binding $CD4^+$ T cell clones exhibited identical CDR3 amino acid sequences although we noted small differences at the level of nucleotide sequences (not shown). For direct measurement of TCR binding affinity, we generated recombinant TCRs from clone #3 and evaluated binding to I-$A^b$$GP_{61–80}$ complexes by surface plasmon resonance (SPR) as detailed in Materials and methods (Fig. 7). SPR measurements at equilibrium demonstrated a K_D of 4.2 μM indicating a relatively high binding affinity as compared to other published $CD4^+$ TCR affinities (Krummel et al., 2000).

Discussion

In this study, we have defined the minimal constraints for the recognition of a dominant, MHC class II-restricted viral determinant. Naturally processed peptides selected by MHC class II molecules demonstrate considerable variability of length (usually 12–26 amino acids) but tend to cluster into families that share a 9 amino acid core segment that interacts with the four major binding pockets of the MHC II moleculev (p1, p4, p6 and p9). Flanking residues of natural peptides can modulate binding affinities and also serve as direct contact residues for TCR recognition (Suri et al., 2006). A recent study has discerned 128 naturally processed I-A^b-

restricted peptides that are 11–21 amino acids in length and derived from both endocytic and cytosolic compartments. Although some studies have begun to employ similar techniques based on tandem mass-spectrometry for the identification of microbial determinants that are processed and presented by MHC II-bearing cells *in vivo* (Meiring et al., 2005; Ovsyannikova et al., 2003), the majority of studies performed to date have relied on measuring the binding affinity of synthetic microbial peptides to recombinant MHC molecules as well as the induction of effector functions in specific responder T cells. The latter approach has been guided, in particular for the mapping of MHC I-restricted epitopes, by the identification of common binding motifs and is usually less effective for prediction of MHC II-restricted determinants. Nevertheless, information about the naturally processed I-A^b-restricted peptide sequences together with the recently solved crystal structure of I-A^b has allowed for the development of a simple scoring matrix (Dongre et al., 2001; Zhu et al., 2003). However, retroactive application of this scoring matrix to the core and related LCMV-GP epitopes identified in this study failed to reveal optimal binding sequences. These observations emphasize that in spite of the comparatively high binding affinities of the dominant LCMV-GP epitope (Krummel et al., 2000), any attempts to predict optimal MHC class II-binding epitope sequences are impaired by the likely usage of alternating peptide binding registers.

The LCMV $GP_{61–80}$ epitope was originally identified by Oxenius et al. (1995) as an immunodominant, I-A^b-restricted determinant derived from the LCMV WE strain. Although LCMV Armstrong differs from LCMV WE by a single N → K substitution in position GP_{63} of this determinant, subsequent work by other groups established that the $GP_{61–80}$ epitope is also dominant for $CD4^+$ T cell responses directed against LCMV Armstrong (Homann et al., 2001; Kamperschroer and Quinn, 1999; Varga and Welsh, 1998a; Varga and Welsh, 1998b; Whitmire et al., 1998). Indeed, we and others have estimated that more than half of the I-A^b-restricted, LCMV Armstrong-specific $CD4^+$ T cell response is directed against this epitope (Homann et al., 2001; Kamperschroer and Quinn, 1999). More recently, Oxenius' group has utilized a truncated GP peptide that lacks the first three C-terminal amino acids ($GP_{64–80}$) to effectively stimulate TCR transgenic $CD4^+$ T cells originally derived from a clone specific for the $GP_{61–80}$ epitope (Wolint et al., 2004). This finding is in agreement with our observation that residues $GP_{61–63}$ are completely dispensable for recognition by $GP_{61–80}$ specific $CD4^+$ T cell clones and also supported by unpublished findings that the GP-specific $CD4^+$ T cell response is unaltered after infection with a variant virus lacking GP residues 59–63 (virus obtained, cloned and sequenced from persistently LCMV Armstrong-infected $D^{b-/-}\times K^{b-/-}$ mice).

Interestingly, our analyses of primary LCMV-specific T cell responses directed against the $GP_{67–77}$ epitope demonstrated the presence of $CD8^+$ T cells that recognize this epitope in the context of D^b. Although a previous publication, using an *in vitro* peptide binding assay, has described a truncated version of the $GP_{67–77}$ epitope ($GP_{70–77}$) as a peptide with high binding affinity to K^b in (van der Most et al., 1998), the use of K^b as a restriction element for the shorter $GP_{70–77}$ epitope has, to the best of our knowledge, not been validated in *ex vivo* experiments. It thus remains possible that the $GP_{67–77}$ and $GP_{70–77}$ epitopes indeed demonstrate restriction by different MHC molecules (D^b vs. K^b, respectively) or that $GP_{70–77}$, similar to the $GP_{33–41}$ epitope, is restricted by both D^b and K^b. Several features are noteworthy in considering binding of $GP_{67–77}$ to H-$2D^b$, a restriction element that has been investigated in great detail. The signature motif has an Asn at P5 and an hydrophobic amino acid at P9 (Meth, Ileu or Leu) (Falk et al., 1991). In the present case, $GP_{67–77}$ is missing the P5 anchor and will have to bind to D^b in a non-classical way (Ostrov et al., 2002). It is likely that $Valine_{77}$ anchors the C-terminus of the peptide, whereas the middle part bulges out, like most 11 mer peptides bound to MHC class I do (Apostolopoulos et al., 2002; Ostrov et al., 2002), and is exposed for T cell recognition. The recognition of one and the same viral determinant by both $CD8^+$ and $CD4^+$ T cells constitutes a unique feature within the LCMV system and should be taken into

consideration for the interpretation of differential $CD4^+$ and $CD8^+$ T cell activities in this model system. For example, $CD8^+$ T cells that recognize the I-A^b-restricted $GP_{61–80}$ epitope have been described in CD4-deficient mice (Pearce et al., 2004; Tyznik et al., 2004). However, this $CD8^+$ T cell response is restricted by I-A^b and its existence was attributed to abnormal T cell development in $CD4^+$ T cell-deficient mice since further experiments indicated that neither wild-type nor acutely CD4-depleted mice mounted an MHC II-restricted $CD8^+$ T cell response following infection with recombinant L. monocytogenes expressing a secreted form of chicken ovalbumin (Tyznik et al., 2004).

Finally, recognition of the same viral determinant by $CD4^+$ and $CD8^+$ T cells may offer an opportunity to optimize immunization strategies utilizing small, defined peptide sequences. As shown by van der Most and colleagues, protection of mice against chronic infection can be achieved even through induction of subdominant $CD8^+$ T cell responses (van der Most et al., 1998) that constitute only a very small fraction of the antiviral $CD8^+$ Tcell population in a natural infection (~2%). To improve the overall effectiveness of these $CD8^+$ T cell responses, the authors utilized a lipidated LCMV $GP_{92–101}$ peptide conjugated to an ovalbumin “helper” epitope (van der Most et al., 1998), a strategy that may be simplified by the use of the $GP_{67–77}$ core peptide and the concurrent induction of genuine virus-specific $CD8^+$ and $CD4^+$ T cell responses.

Materials and methods

Mice and virus

C57BL/6 (H-2^b, Thy1.2^+) and congenic B6.PL (Thy1.1^+) mice were purchased from the closed vivarium breeding colony at The Scripps Research Institute. Mice lacking D^b, K^b or $D^b \times K^b$ expression were obtained from Taconic, Hudson NY. Origin, growth and titration of lymphocytic choriomeningitis virus (LCMV) Armstrong clone 53b have been described (Homann et al., 1998). Eight to ten week old C57BL/6 mice were infected with a single intraperitoneal dose of 10^5 plaque forming units LCMV Armstrong.

$CD4^+$ T cell lines and clones

LCMV $GP_{61–80}$-specific, I-A^b-restricted $CD4^+$ T cell lines and clones were obtained from C57BL/6 mice 13 days after infection with 1.5×10^5 pfu LCMVArmstrong i.p. Spleens were harvested, single cell suspensions prepared, red blood cell lysed and $CD8^+$ T cells depleted with antibody-coated magnetic beads as described (Berger et al., 2000). Cell counts were adjusted to 5×10^6 cells/ml in cloning medium (RPMI 1640 supplemented with 8% FCS, 1% penicillin/streptomycin, 1 mM L-glutamine and 50 units of human IL-2) supplemented with 1 μg/ml $GP_{61–80}$ peptide, and plated in 24-well tissue culture plates. After 1 week, cultures were supplemented regularly with “feeder cells” (irradiated C57BL/6 spleen cells) as needed, intermittently rested by withdrawal of LCMV $GP_{61–80}$ peptide and specific $CD4^+$ T cell lines and clones established by limiting dilution techniques (Anderson et al., 1985).

Flow cytometry

For detection of intracellular IFNγ, rested cell lines and clones as well as primary T cells were restimulated for 5 h with peptides (1–5 μg/ml) prior to surface and intracellular stains as detailed elsewhere (Homann et al., 2001). Preparation and use of I-A^b tetramers and tetramer-liposomes have been described (Homann et al., 2001; Mallet-Designé et al., 2003). In this study, tetramers (20 μg/ml; 40 μl volume) were incubated with cells at room temperature for 45–75 min prior to addition of antibody reagents, further incubation (20 min), washes and immediate acquisition on a BD FACSCalibur flow cytometer. For quantitation of expression levels, we used the normalized geometric mean of fluorescence intensity (GMFI, calculated by dividing GMFI of the experimental stain by GMFI of corresponding control stain). Functional avidities were

determined as described (Homann et al., 2006; Homann et al., 2002). For determination of TCR Vβ usage, we employed a kit comprising a panel of available TCR Vβ-specific antibodies (BDPharmingen).

CTL assay

Direct *ex vivo* CTL activity was analyzed 7 days after LCMV infection in a standard ^{51}Cr release assay as described (Homann et al., 1998).

Sequencing and recombinant expression of TCRs

The cDNA for the α and β chain of TCR for CD4 T cell clones #3 and #31 was obtained by RT-PCR using Ready-To-Go RT-PCR beads (Amersham Pharmacia Biotech, Piscataway, NJ) according to the manufacturer's instructions. In brief, RNA isolated from clones was used for cDNA synthesis and PCR amplification. PCR products were subcloned into pCR2.1-TOPO cloning vector (Invitrogen, Carlsbad, CA), sequenced and subcloned into the metallothionein promoter-based fly expression vector pRMHa3 (Fremont et al., 1992). The final constructs coded for the α1α2 and β1β2 domains, respectively, followed by a linker sequence (SSADL), a thrombin site (LVPRGS), a leucine zipper (acidic for the α chain, basic for the β chain) (Scott et al., 1996) and a hexahistidine tag. Vectors were transfected into SC2 cells and stable cell lines and clones were established. Soluble TCRs were purified from culture supernatants as described (Garcia et al., 1997; Matsumura et al., 1992; Scott et al., 1998).

Surface plasmon resonance

A BIACORE 2000 instrument was used to determine interactions between purified pMHC (peptide:MHC) complexes and recombinant TCR molecules as described (Mallet-Designé et al., 2003). In brief, pMHC complexes or TCRs were immobilized by amine coupling chemistry on a CM5 research grade sensor chip. Successive injections of pMHC complexes or TCRs were performed in filtered and degassed PBS buffer at a flow rate of 20 μl/min at concentrations of 20, 10, 5, 2.5, and 1.25 μM. In all experiments, irrelevant TCR molecules or irrelevant pMHC (I-A^b/ova) were used as negative control and subtracted from experimental sensorgrams. On- and off- rates were obtained by non-linear curve fitting of subtracted curves using the 1:1 Langmuir binding model using the BIAevaluation program (version 3.0.2).

Statistical analysis

Data handling, analysis and graphic representation were performed using Prism 4.0a (GraphPad Software, San Diego, California); *p* values were calculated by Student's *t*-test.

Acknowledgements

This is publication number 17545-NP from the Molecular and Integrative Neurosciences Department and Department of Infectology, The Scripps Research Institute, La Jolla, CA. This work was supported in part by NIH 1R21 AG026518-01 (D.H), AI009484 (M.B.A.O.), NIH training grant 5T32 AI007244-23 (D.B.) and NIH DK055037 (L.T.).

References

Anderson J, Byrne JA, Schreiber R, Patterson S, Oldstone MB. Biology of cloned cytotoxic T lymphocytes specific for lymphocytic choriomeningitis virus: clearance of virus and in vitro properties. J Virol 1985;53(2):552–560. [PubMed: 3918175]

Apostolopoulos V, Yu M, Corper AL, Li W, McKenzie IF, Teyton L, Wilson IA, Plebanski M. Crystal structure of a non-canonical high affinity peptide complexed with MHC class I: a novel use of alternative anchors. J Mol Biol 2002;318(5):1307–1316. [PubMed: 12083519]

Appay V. The physiological role of cytotoxic CD4 (+) T-cells: the holy grail? Clin Exp Immunol 2004;138 (1):10–13. [PubMed: 15373899]

Belkaid Y, Rouse BT. Natural regulatory T cells in infectious disease. Nat Immunol 2005;6(4):353–360. [PubMed: 15785761]

Berger DP, Homann D, Oldstone MB. Defining parameters for successful immunocytotherapy of persistent viral infection. Virology 2000;266(2):257–263. [PubMed: 10639312]

Bevan MJ. Helping the CD8 (+) T-cell response. Nat Rev Immunol 2004;4(8):595–602. [PubMed: 15286726]

Burton DR. Opinion: antibodies, viruses and vaccines. Nat Rev Immunol 2002;2(9):706–713. [PubMed: 12209139]

Corper AL, Stratmann T, Apostolopoulos V, Scott CA, Garcia KC, Kang AS, Wilson IA, Teyton L. A structural framework for deciphering the link between I-Ag7 and autoimmune diabetes. Science 2000;288(5465):505–511. [PubMed: 10775108]

Dittmer U, He H, Messer RJ, Schimmer S, Olbrich AR, Ohlen C, Greenberg PD, Stromnes IM, Iwashiro M, Sakaguchi S, Evans LH, Peterson KE, Yang G, Hasenkrug KJ. Functional impairment of CD8 (+) T cells by regulatory T cells during persistent retroviral infection. Immunity 2004;20(3):293–303. [PubMed: 15030773]

Dongre AR, Kovats S, deRoos P, McCormack AL, Nakagawa T, Paharkova-Vatchkova V, Eng J, Caldwell H, Yates JR, Rudensky AY. In vivo MHC class II presentation of cytosolic proteins revealed by rapid automated tandem mass spectrometry and functional analyses. Eur J Immunol 2001;31(5): 1485–1494. [PubMed: 11465105]

Falk K, Rotzschke O, Stevanovic S, Jung G, Rammensee HG. Allele-specific motifs revealed by sequencing of self-peptides eluted from MHC molecules. Nature 1991;351(6324):290–296. [PubMed: 1709722]

Fremont DH, Matsumura M, Stura EA, Peterson PA, Wilson IA. Crystal structures of two viral peptides in complex with murine MHC class I H-2Kb. Science 1992;257(5072):919–927. [PubMed: 1323877]

Gairin JE, Mazarguil H, Hudrisier D, Oldstone MB. Optimal lymphocytic choriomeningitis virus sequences restricted by H-2Db major histocompatibility complex class I molecules and presented to cytotoxic T lymphocytes. J Virol 1995;69(4):2297–2305. [PubMed: 7533855]

Garcia KC, Tallquist MD, Pease LR, Brunmark A, Scott CA, Degano M, Stura EA, Peterson PA, Wilson IA, Teyton L. Alphabeta T cell receptor interactions with syngeneic and allogeneic ligands: affinity measurements and crystallization. Proc Natl Acad Sci U S A 1997;94(25):13838–13843. [PubMed: 9391114]

Homann D. Immunocytotherapy. Curr Top Microbiol Immunol 2002;263:43–65. [PubMed: 11987819]

Homann D, Tishon A, Berger DP, Weigle WO, von Herrath MG, Oldstone MB. Evidence for an underlying CD4 helper and CD8 T-cell defect in B-cell-deficient mice: failure to clear persistent virus infection after adoptive immunotherapy with virus-specific memory cells from muMT/muMT mice. J Virol 1998;72(11):9208–9216. [PubMed: 9765468]

Homann D, Teyton L, Oldstone MB. Differential regulation of antiviral T-cell immunity results in stable CD8+ but declining CD4+ T-cell memory. Nat Med 2001;7(8):913–919. [PubMed: 11479623]

Homann D, Jahreis A, Wolfe T, Hughes A, Coon B, van Stipdonk MJ, Prilliman KR, Schoenberger SP, von Herrath MG. CD40L blockade prevents autoimmune diabetes by induction of bitypic NK/DC regulatory cells. Immunity 2002;16(3):403–415. [PubMed: 11911825]

Homann D, Dummer W, Wolfe T, Rodrigo E, Theofilopoulos AN, Oldstone MB, von Herrath MG. Lack of intrinsic ctla-4 expression has minimal effect on regulation of antiviral T-cell immunity. J Virol 2006;80(1):270–280. [PubMed: 16352552]

Hudrisier D, Oldstone MB, Gairin JE. The signal sequence of lymphocytic choriomeningitis virus contains an immunodominant cytotoxic T cell epitope that is restricted by both H-2D (b) and H-2K (b) molecules. Virology 1997;234(1):62–73. [PubMed: 9234947]

Jenkins MK, Khoruts A, Ingulli E, Mueller DL, McSorley SJ, Reinhardt RL, Itano A, Pape KA. In vivo activation of antigen-specific CD4 T cells. Annu Rev Immunol 2001;19:23–45. [PubMed: 11244029]

Kamperschroer C, Quinn DG. Quantification of epitope-specific MHC class-II-restricted T cells following lymphocytic choriomeningitis virus infection. Cell Immunol 1999;193(2):134–146. [PubMed: 10222055]

Klavinskis LS, Whitton JL, Joly E, Oldstone MB. Vaccination and protection from a lethal viral infection: identification, incorporation, and use of a cytotoxic T lymphocyte glycoprotein epitope. Virology 1990;178(2):393–400. [PubMed: 1699348]

Krummel M, Wulfing C, Sumen C, Davis MM. Thirty-six views of T-cell recognition. Philos Trans R Soc London, Ser B Biol Sci 2000;355(1400):1071–1076. [PubMed: 11186308]

Lenz DC, Kurz SK, Lemmens E, Schoenberger SP, Sprent J, Oldstone MB, Homann D. IL-7 regulates basal homeostatic proliferation of antiviral CD4+T cell memory. Proc Natl Acad Sci U S A 2004;101 (25):9357–9362. [PubMed: 15197277]

Mallet-Designé VI, Stratmann T, Homann D, Carbone F, Oldstone MB, Teyton L. Detection of low-avidity CD4+ T cells using recombinant artificial APC: following the anti-ovalbumin immune response. J Immunol 2003;170(1):123–131. [PubMed: 12496391]

Matsumura M, Saito Y, Jackson MR, Song ES, Peterson PA. In vitro peptide binding to soluble empty class I major histocompatibility complex molecules isolated from transfected *Drosophila melanogaster* cells. J Biol Chem 1992;267(33):23589–23595. [PubMed: 1331092]

McHeyzer-Williams M, McHeyzer-Williams L, Panus J, Pogue-Caley R, Bikah G, Driver D, Eisenbraun M. Helper T-cell-regulated B-cell immunity. Microbes Infect 2003;5(3):205–212. [PubMed: 12681409]

Meiring HD, Kuipers B, van Gaans-van den Brink JA, Poelen MC, Timmermans H, Baart G, Brugghe H, van Schie J, Boog CJ, de Jong AP, van Els CA. Mass tag-assisted identification of naturally processed HLA class II-presented meningococcal peptides recognized by CD4+ T lymphocytes. J Immunol 2005;174(9):5636–5643. [PubMed: 15843563]

Mittrucker HW, Kaufmann SH. Mini-review: regulatory T cells and infection: suppression revisited. Eur J Immunol 2004;34(2):306–312. [PubMed: 14768034]

Norris PJ, Rosenberg ES. CD4 (+) T helper cells and the role they play in viral control. J Mol Med 2002;80 (7):397–405. [PubMed: 12110945]

Oldstone MB, Whitton JL, Lewicki H, Tishon A. Fine dissection of a nine amino acid glycoprotein epitope, a major determinant recognized by lymphocytic choriomeningitis virus-specific class I-restricted H-2Db cytotoxic T lymphocytes. J Exp Med 1988;168(2):559–570. [PubMed: 2457647]

Ostrov DA, Roden MM, Shi W, Palmieri E, Christianson GJ, Mendoza L, Villaflor G, Tilley D, Shastri N, Grey H, Almo SC, Roopenian D, Nathenson SG. How H13 histocompatibility peptides differing by a single methyl group and lacking conventional MHC binding anchor motifs determine self-nonself discrimination. J Immunol 2002;168(1):283–289. [PubMed: 11751972]

Ovsyannikova IG, Johnson KL, Naylor S, Muddiman DC, Poland GA. Naturally processed measles virus peptide eluted from class II HLA-DRB1*03 recognized by T lymphocytes from human blood. Virology 2003;312(2):495–506. [PubMed: 12919753]

Oxenius A, Bachmann MF, Ashton-Rickardt PG, Tonegawa S, Zinkernagel RM, Hengartner H. Presentation of endogenous viral proteins in association with major histocompatibility complex class II: on the role of intracellular compartmentalization, invariant chain and the TAP transporter system. Eur J Immunol 1995;25(12):3402–3411. [PubMed: 8566030]

Pearce EL, Shedlock DJ, Shen H. Functional characterization of MHC class II-restricted CD8+CD4− and CD8−CD4− T cell responses to infection in CD4−/− mice. J Immunol 2004;173(4):2494–2499. [PubMed: 15294964]

Schulz M, Aichele P, Vollenweider M, Bobe FW, Cardinaux F, Hengartner H, Zinkernagel RM. Major histocompatibility complex-dependent T cell epitopes of lymphocytic choriomeningitis virus nucleoprotein and their protective capacity against viral disease. Eur J Immunol 1989;19(9):1657–1667. [PubMed: 2477254]

Scott CA, Garcia KC, Carbone FR, Wilson IA, Teyton L. Role of chain pairing for the production of functional soluble IA major histo-compatibility complex class II molecules. J Exp Med 1996;183(5): 2087–2095. [PubMed: 8642319]

Scott CA, Peterson PA, Teyton L, Wilson IA. Crystal structures of two I-Ad-peptide complexes reveal that high affinity can be achieved without large anchor residues. Immunity 1998;8(3):319–329. [PubMed: 9529149]

Seder RA, Ahmed R. Similarities and differences in CD4+ and CD8+ effector and memory T cell generation. Nat Immunol 2003;4(9):835–842. [PubMed: 12942084]

Seder RA, Paul WE. Acquisition of lymphokine-producing phenotype by CD4+ T cells. Annu Rev Immunol 1994;12:635–673. [PubMed: 7912089]

Sprent J, Surh CD. T cell memory. Annu Rev Immunol 2002;20:551–579. [PubMed: 11861612]

Suri A, Lovitch SB, Unanue ER. The wide diversity and complexity of peptides bound to class II MHC molecules. Curr Opin Immunol 2006;18(1):70–77. [PubMed: 16316750]

Tyznik AJ, Sun JC, Bevan MJ. The CD8 population in CD4-deficient mice is heavily contaminated with MHC class II-restricted T cells. J Exp Med 2004;199(4):559–565. [PubMed: 14769854]

van der Most RG, Murali-Krishna K, Whitton JL, Oseroff C, Alexander J, Southwood S, Sidney J, Chesnut RW, Sette A, Ahmed R. Identification of Db- and Kb-restricted subdominant cytotoxic T-cell responses in lymphocytic choriomeningitis virus-infected mice. Virology 1998;240(1):158–167. [PubMed: 9448700]

van der Most RG, Murali-Krishna K, Lanier JG, Wherry EJ, Puglielli MT, Blattman JN, Sette A, Ahmed R. Changing immunodominance patterns in antiviral CD8 T-cell responses after loss of epitope presentation or chronic antigenic stimulation. Virology 2003;315(1):93–102. [PubMed: 14592762]

Varga SM, Welsh RM. Detection of a high frequency of virus-specific CD4+ T cells during acute infection with lymphocytic choriomeningitis virus. J Immunol 1998a;161(7):3215–3218. [PubMed: 9759834]

Varga SM, Welsh RM. Stability of virus-specific CD4+ T cell frequencies from acute infection into long term memory. J Immunol 1998b;161(1):367–374. [PubMed: 9647245]

Varga SM, Welsh RM. High frequency of virus-specific interleukin-2-producing CD4 (+) T cells and Th1 dominance during lymphocytic choriomeningitis virus infection. J Virol 2000;74(9):4429–4432. [PubMed: 10756059]

Whitmire JK, Asano MS, Murali-Krishna K, Suresh M, Ahmed R. Long-term CD4 Th1 and Th2 memory following acute lymphocytic choriomeningitis virus infection. J Virol 1998;72(10):8281–8288. [PubMed: 9733872]

Whitmire JK, Benning N, Whitton JL. Precursor frequency, nonlinear proliferation, and functional maturation of virus-specific CD4+ T cells. J Immunol 2006;176(5):3028–3036. [PubMed: 16493061]

Whitton, JL.; Oldstone, MB. The immune response to viruses. In: Knipe, D.; Howley, P.; Griffin, D.; Lamb, R.; Martin, M.; Strauss, S., editors. Field's Virology. 4. Lippincott Williams; Wilkins, Philadelphia: 2001. p. 285-320.

Wolint P, Betts MR, Koup RA, Oxenius A. Immediate cytotoxicity but not degranulation distinguishes effector and memory subsets of CD8+ T cells. J Exp Med 2004;199(7):925–936. [PubMed: 15051762]

Zhu Y, Rudensky AY, Corper AL, Teyton L, Wilson IA. Crystal structure of MHC class II I-Ab in complex with a human CLIP peptide: prediction of an I-Ab peptide-binding motif. J Mol Biol 2003;326(4):1157–1174. [PubMed: 12589760]

Zinkernagel RM. On differences between immunity and immunological memory. Curr Opin Immunol 2002;14(4):523–536. [PubMed: 12088689]

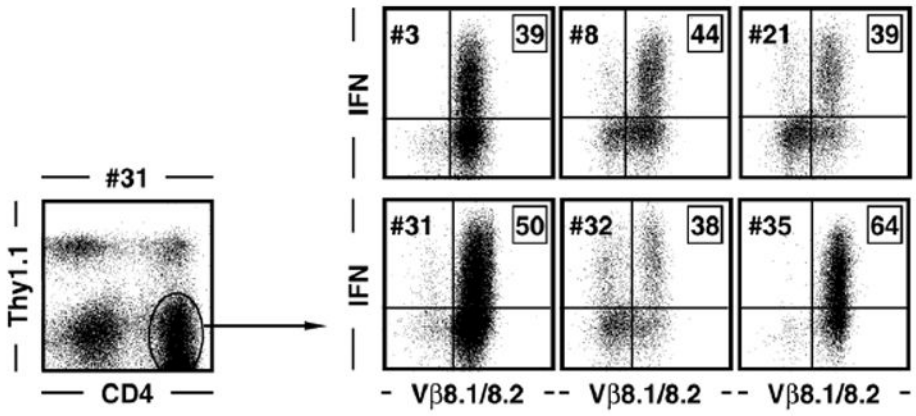

Fig. 1. Establishment and functional characterization of $GP_{61–80}$-specific $CD4^+$ T cell lines and clones

$CD4^+$ T cell lines and clones were generated as detailed in Materials and methods. To evaluate antigen-specific T cell function and TCR usage, cells were rested by antigen withdrawal, supplemented with congenic ($Thy1.1^+$) spleen cells to provide a source for MHC class II-restricted antigen presentation and stimulated for 5 h with $GP_{61–80}$ peptide. Cells were subsequently stained for CD4, Thy1.1 and TCR Vβ8.1/8.2 as well as intracellular IFNγ. Dot plots on the right are gated on Thy1.1-negative $CD4^+$ T cells as indicated by the exemplary dot plot on the left; boxed values indicate percentages of $IFN\gamma^+$ gated $CD4^+$ T cells.

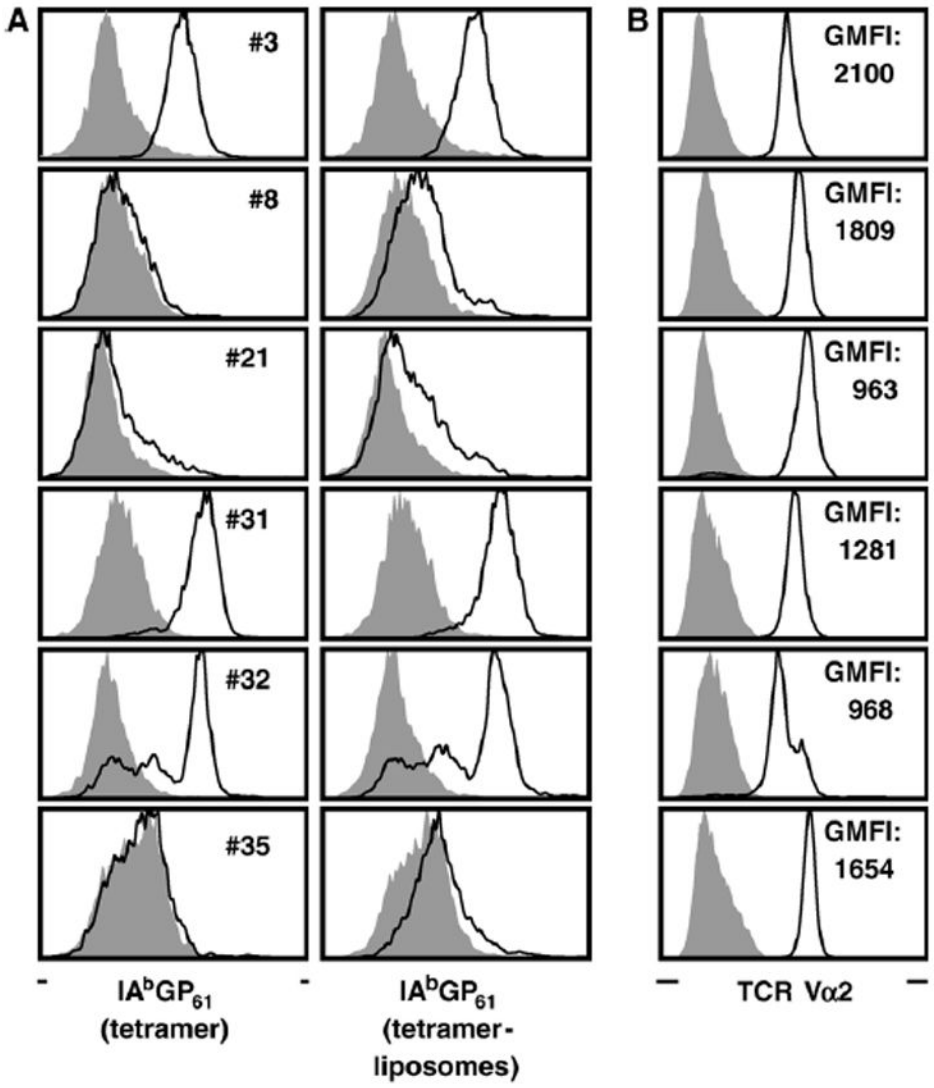

Fig. 2. T cell receptor usage by $GP_{61–80}$-specific $CD4^+$ T cell clones/lines

(A) $CD4^+$ T cell clones/lines were rested in the absence of antigen and stained for CD4 as well as tetramers (left column) or tetramer-liposomes (right column) as detailed in Materials and methods. Black tracings indicate staining with I-$A^bGP_{61–80}$ tetramers or tetramer-liposomes; gray histograms indicate control stains with I-$A^bOVA_{323–339}$ tetramers or tetramer-liposomes. (B) In parallel stains, TCR expression levels were determined by staining for TCR Vα2 (black tracing); for control stains (gray histograms) cells were stained for TCR Vα8. Values represent the geometric mean of fluorescence intensity (GMFI) of Vα2 stains.

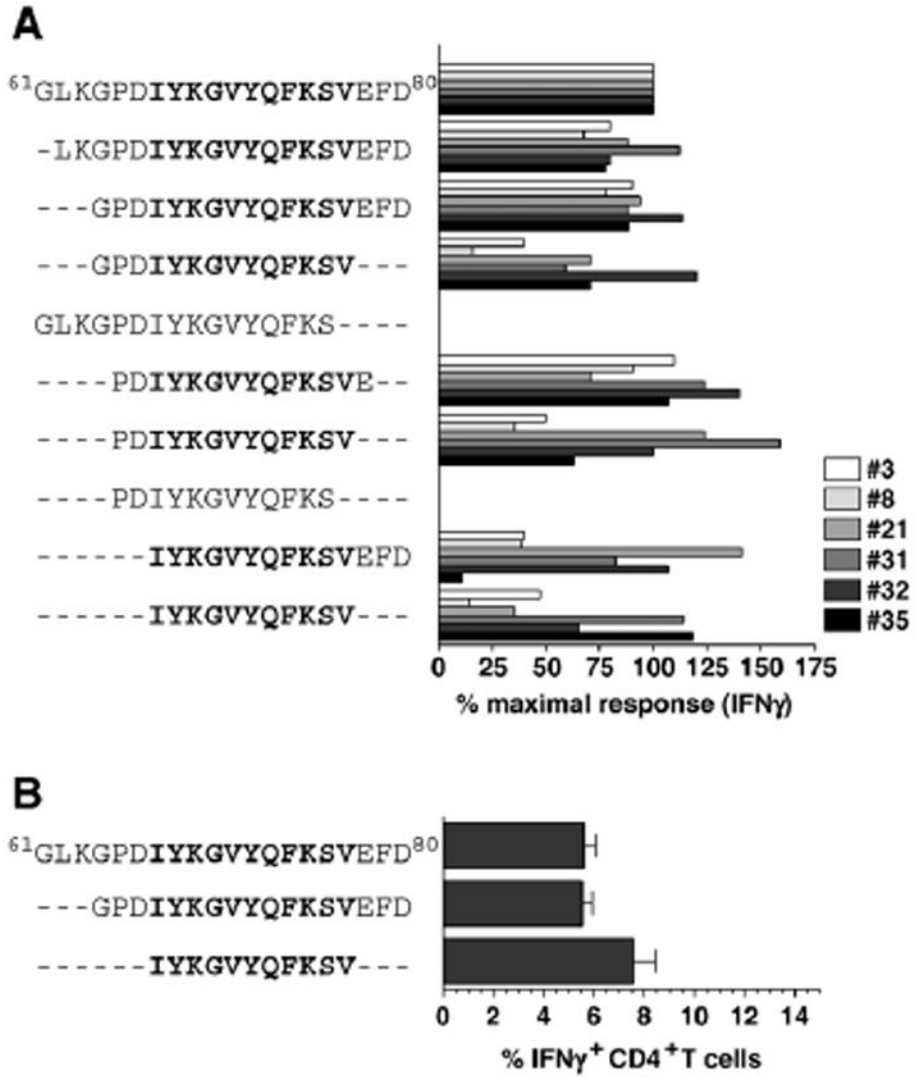

Fig. 3. Identification of the minimal $GP_{61–80}$ binding constraints

(A) $CD4^+$ T cell clones and lines #3, #8, #21, #31, #32 and #35 were rested by antigen withdrawal, restimulated with indicated peptides and stained for intracellular IFN. The percentage of $IFN\gamma^+$ cells after stimulation with the native $GP_{61–80}$ peptide of individual cell lines or clones was set at 100% and the values after stimulation with truncated peptides were calculated accordingly. All clones/cell lines (#3, #8, #21, #31, #32 and #35) were tested in parallel. Data for individual clones/cell lines obtained in two separate experiments were combined according to peptide sequences used for stimulation; no statistical analysis was performed as each value consists of only 2 data points. (B) Eight days after LCMV infection of B6 mice, spleen cells were restimulated with indicated peptides and frequencies of epitope-specific $CD4^+$ T cells were determined by intracellular IFNγ staining (3 mice/experiment; values indicate SEM of one out of four independent experiments).

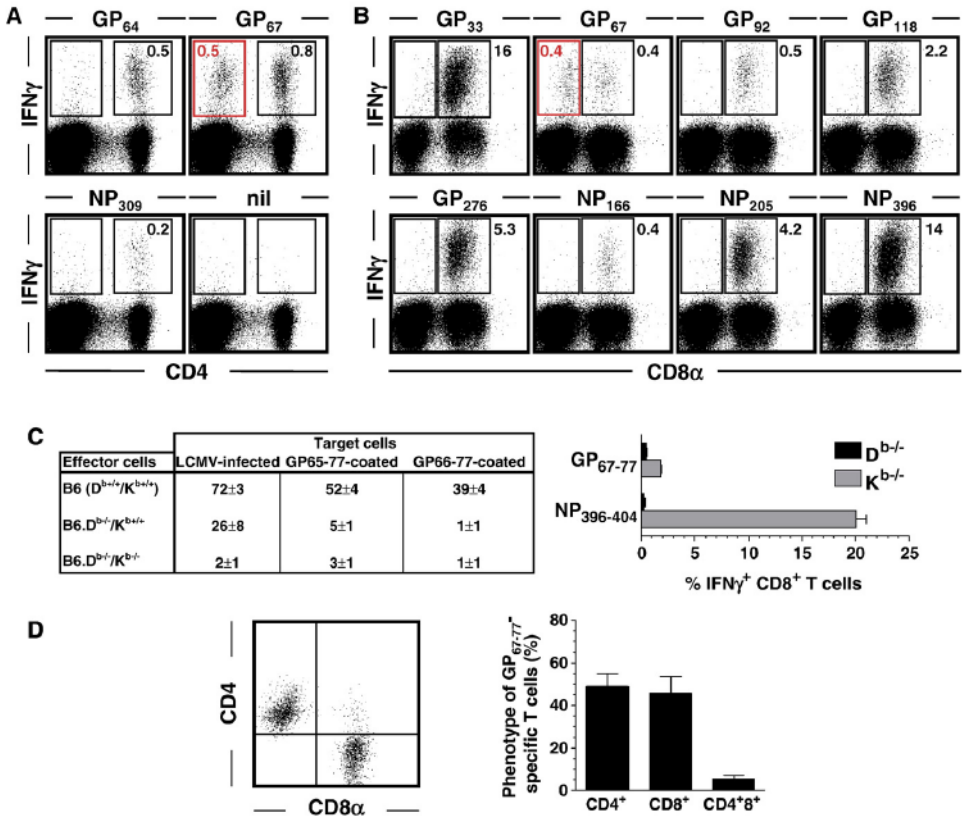

Fig. 4. Recognition of the $GP_{67–77}$ core epitope by both virus-specific $CD4^+$ and $CD8^+$ T cells

Spleen cells harvested from B6 mice infected with $1.5×10^5$ pfu LCMV Armstrong i.p. 8 days earlier were stimulated for 5 h with the indicated peptides (nil: no peptide) and analyzed for induced IFNγ expression (Plots are gated on spleen cells according to FSC/SSC properties. Values indicate percentages of $IFN\gamma^+$ cells in indicated rectangular gates; absence of values in some gates refers to background staining levels of <0.1%). (A) Analysis of specific $CD4^+$ T cell responses demonstrates IFNγ induction in CD4-negative cells only after stimulation with GP_{67} (red gate) but not GP_{61} or NP_{309} peptides. (B) Parallel analyses of IFNγ production by $CD8^+$ T cells revealed induction of IFNγ in CD8-negative cells only after stimulation with GP_{67} peptide (red gate). (C) Left panel: Seven days after LCMV infection of B6 ($D^{b+/+}$/$K^{b+/+}$), B6.$D^{b-/-}$/$K^{b+/+}$ and B6.$D^{b-/-}$/$K^{b-/-}$ mice, spleen cell suspensions were tested for specific epitope-specific CTL activity using virus-infected or peptide-coated target cells in a conventional 5 h *ex vivo* CTL assay. Specific lysis for effector:target cell cultures at a ratio of 50:1 is shown; values indicate the percentage (SEM) of ^{51}Cr release from target cells. Note that lack of D^b expression abolishes killing of $GP_{65–77}$ and $GP_{67–77}$ coated target cells. Right panel: Eight days after infection of B6.$D^{b-/-}$/$K^{b+/+}$ and B6.$D^{b+/+}$/$K^{b-/-}$ mice, epitope-specific $CD8^+$T cell responses were quantified by peptide restimulation and intracellular IFNg staining; displayed are the percentages of epitope-specific $CD8^+$T cells (3 mice/group, SEM). Note that lack of D^b expression abolishes $GP_{67–77}$-induced IFNg production. The $NP_{396–404}$-specific IFNg response has been included as a control for a *bona fide* D^b-restricted $CD8^+$T cell response. (D) Phenotype of $GP_{67–77}$-specific T cells. Eight days after LCMV infection of B6 mice, spleen cells were restimulated with $GP_{67–77}$ peptide and stained for CD8α, CD4 and intracellular IFNγ. The dot plot is gated on $IFN\gamma^+$T cells indicating the distribution of $GP_{67–77}$-specific T cells among $CD8^+$ and $CD4^+$ subsets. The adjacent bar diagram summarizes these findings (3 mice/experiment; 3 independent experiments).

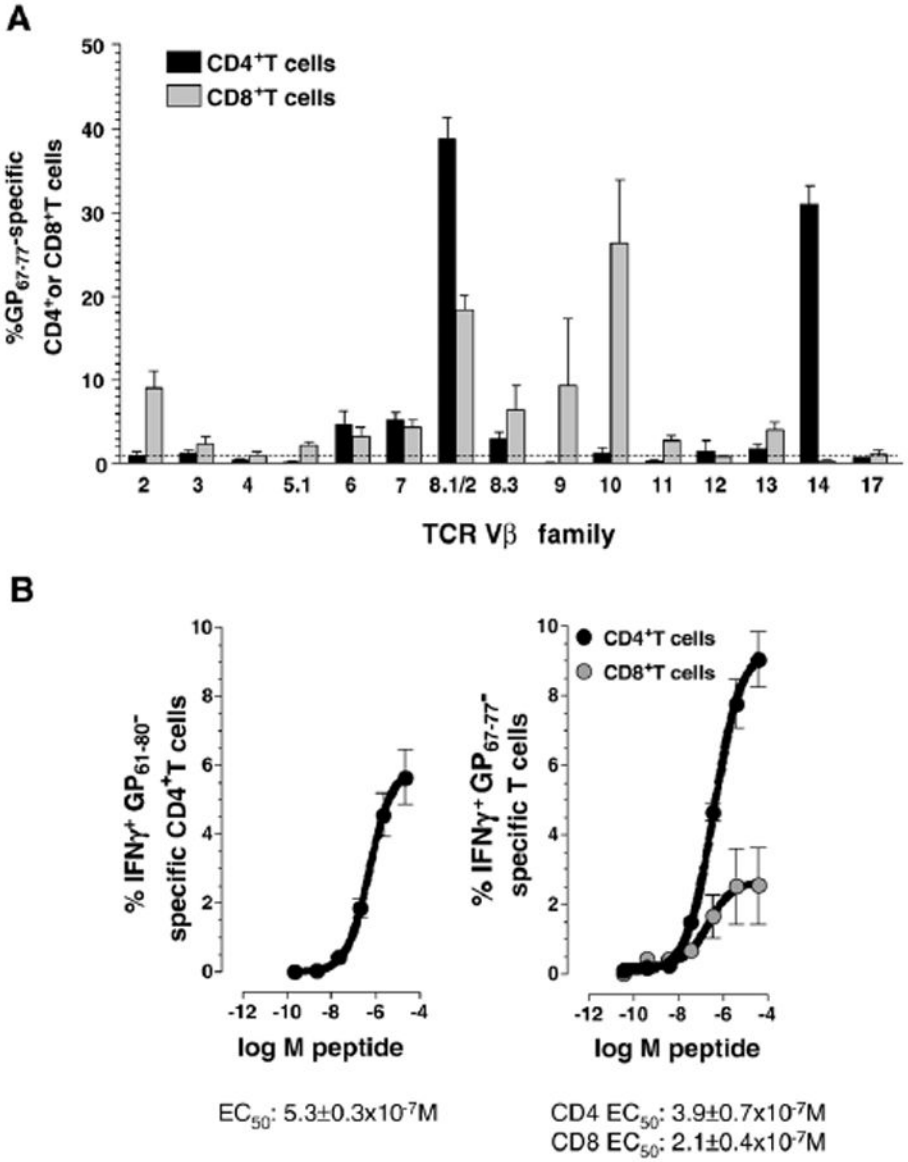

Fig. 5. TCRVβ usage and functional avidities of $GP_{67–77}$-specific $CD4^+$ and $CD8^+$ effector Tcells

(A) Effector spleen cells (8 days after LCMV) were restimulated for 5 h with $GP_{67–77}$ peptide and stained for surface markers (CD8, CD4, TCRVβ subfamily) and intracellular IFNγ. Bar diagrams display relative distribution of TCRVβ usage by $GP_{67–77}$-specific ($IFN\gamma^+$) $CD4^+$ (black) and $CD8^+$ (gray) Tcells. The dotted line indicates the level of non-specific background staining. Bars indicate mean± SE from 2 independent experiments using 2–3 mice each. (B) Functional avidities were determined by culture of effector spleen cell suspension with graded dosages of $GP_{61–80}$ or $GP_{67–77}$ peptide and plotting of $IFN\gamma^+$ effector T cell frequencies (mean ±SE) against the peptide concentration used for restimulation (data from 1 of 3 independent experiments using 2–3 mice each). Values listed below the graphs represent the EC50 for indicated peptide specificities and specific Tcells, i.e. the peptide concentration required to elicit detectable IFNγ induction in half of the $GP_{61–80}^-$ (left) and $GP_{67–77}^-$ specific (right) $CD4^+$ or $CD8^+$ Tcell populations (mean±SE, 1 of 3 independent experiments). Although EC50 values of $GP_{67–77}^-$ specific $CD4^+$ and $CD8^+$ T cells as well as of $GP_{61–80}^-$ and $GP_{67–77}$-specific

$CD4^+$ T cells were not significantly different, $GP_{67–77}$-specific $CD8^+$ T cells exhibited a lower EC_{50} when compared to $GP_{61–80}$-specific $CD4^+$ T cells (p=0.0085).

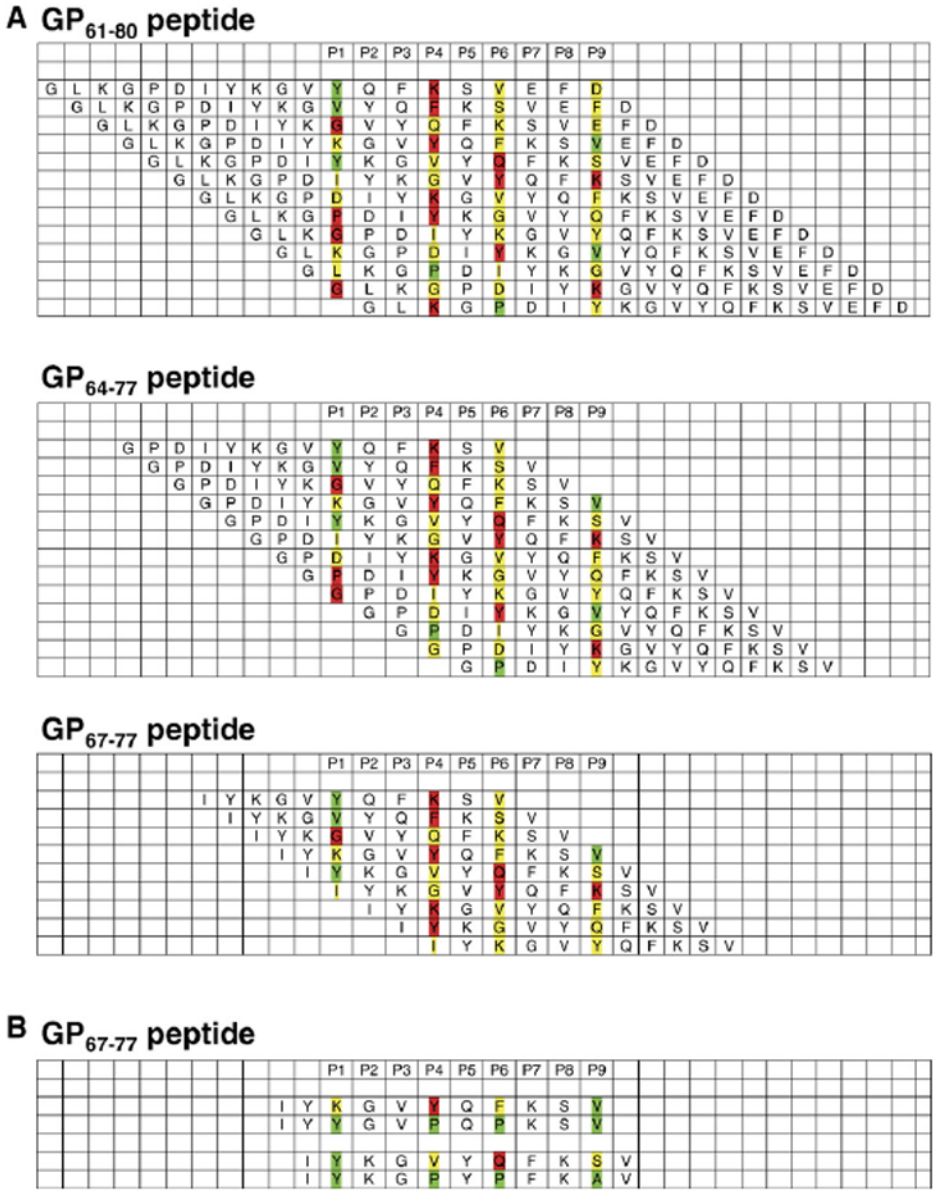

Fig. 6. Fitting of dominant LCMV-GP epitope sequences to I-A^b

P1 to P9 signify I-A^b binding pockets. The interactions of individual amino acids with I-A^b binding pockets are differentiated according to optimal (green), neutral (yellow) and unfavorable (red) binding properties. (A) Potential alignments and registers for $GP_{61–80}$, $GP_{64–77}$ and $GP_{67–77}$. The shortening of the original peptide was done first using each alignment. (B) Then, the minimal peptide, $GP_{67–77}$, was modified in 2 registers to try to increase affinity and T cell response by introducing optimal anchor residues.

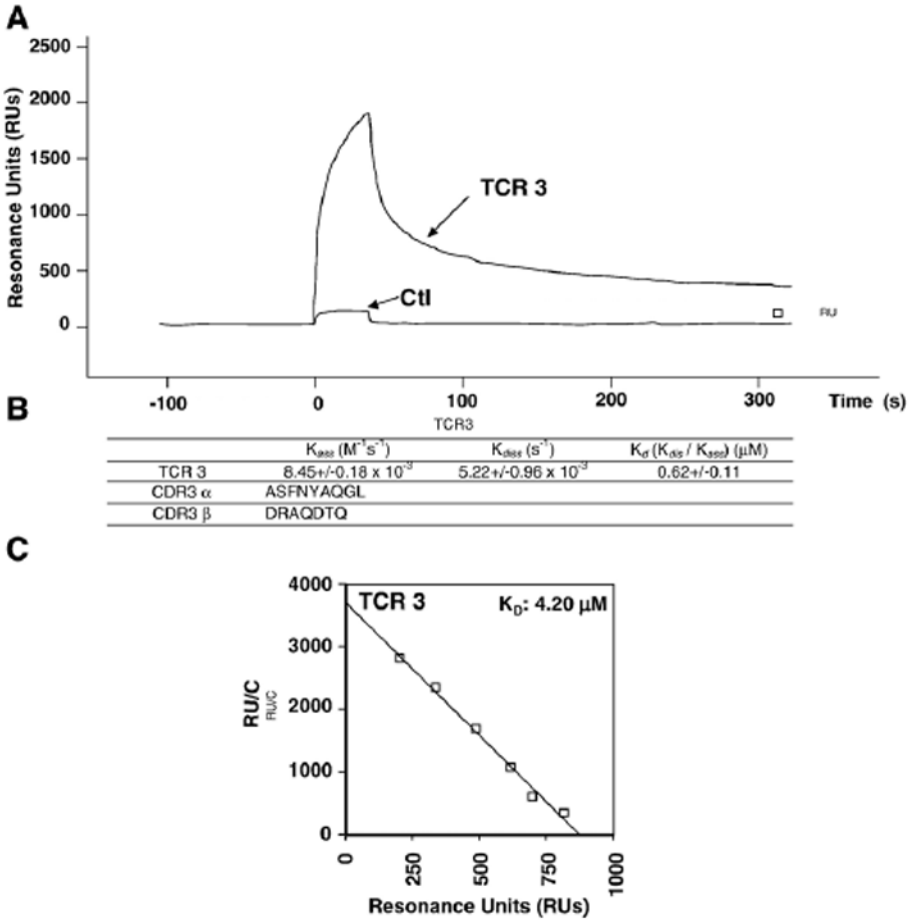

	K_{ass} ($M^{-1}s^{-1}$)	K_{diss} (s^{-1})	K_d (K_{dis} / K_{ass}) (µM)
TCR 3	8.45+/-0.18 x 10^{-3}	5.22+/-0.96 x 10^{-3}	0.62+/-0.11
CDR3 α	ASFNYAQGL		
CDR3 β	DRAQDTQ		

Fig. 7. Determining the affinity of TCR #3

Recombinant T cell receptors based on sequences derived from clone #3 were constructed as detailed in Materials and methods and tested for binding to I-$A^b$$GP_{61–80}$ complexes by plasmon surface resonance. TCR3: recombinant $GP_{61–80}$-specific TCR obtained from clone #3; Ctl: control.